

Chemical Bonding Topology of Ternary Transition Metal-Centered Bismuth Cluster Halides: From Molecules to Metals

R. Bruce King*

Department of Chemistry, University of Georgia, Athens, Georgia 30602

Received June 25, 2003

The bismuth polyhedra in ternary transition metal-centered bismuth cluster halides may form discrete molecules or ions, infinite chains, and/or infinite layers. The chemical bonding in many of these diverse structures is related to that in deltahedral boranes exhibiting three-dimensional aromaticity by replacing the multicenter core bond in the boranes with two-center two-electron (2c–2e) bonds from the central transition metal to the nearest neighbor bismuth vertices. Examples of discrete molecules or ions include octahedral $\text{MBi}_6(\mu\text{-X})_{12}^{z-}$ ($\text{X} = \text{Br}, \text{I}; \text{M} = \text{Rh}, \text{Ir}, z = 3; \text{M} = \text{Ru}, z = 4$) with exclusively 2c–2e bonds and pentagonal bipyramidal RhBi_7Br_8 with a 5c–4e bond in the equatorial pentagonal plane indicative of Möbius aromaticity. The compound $\text{Ru}_3\text{Bi}_{24}\text{Br}_{20}$ contains a more complicated discrete bismuth cluster ion $\text{Ru}_2\text{Bi}_{17}(\mu\text{-Br})_4^{5+}$, which can be dissected into a RuBi_5 *closo* octahedron and a RuBi_8 *nido* capped square antiprism bridged by a $\text{Ru}_2\text{Bi}_4(\mu\text{-Br})_4$ structural unit. In RuBi_4X_2 ($\text{X} = \text{Br}, \text{I}$), the same $\text{Ru}_2\text{Bi}_4(\mu\text{-Br})_4$ structural unit bridges Bi_4 squares similar to those found in the known Zintl ion Bi_4^{2-} to give infinite chains of Ru_2Bi_4 octahedra. The electron counts of the RuBi_5 , RuBi_8 , and Ru_2Bi_4 polyhedra in these structures follow the Wade–Mingos rules. A different infinite chain structure is constructed from fused $\text{RhBi}_{7/2}\text{Bi}$ bicapped trigonal prisms in $\text{Rh}_2\text{Bi}_9\text{Br}_3$. This $\text{Rh}_2\text{Bi}_9\text{Br}_3$ structure can alternatively be derived from alternating $\text{Rh}_{2/2}\text{Bi}_4$ octahedra and $\text{Rh}_{2/2}\text{Bi}_5$ pentagonal bipyramids with electron counts obeying the Wade–Mingos rules. Related chemical bonding principles appear to apply to more complicated layer structures such as $\text{Pt}_3\text{Bi}_{13}\text{I}_7$ containing Kagomé nets of $\text{PtBi}_{8/2}$ cubes and $\text{Ni}_4\text{Bi}_{12}\text{X}_3$ containing linked chains of $\text{NiBi}_{6/3}\text{Bi}$ capped trigonal prisms.

1. Introduction

A topic of interest in recent years has been the relationship between molecular metal clusters and bulk metals. In the cluster chemistry of the early transition metals, the author has investigated the effect on the chemical bonding in going from the discrete molecular octahedral cluster $\text{Mo}_6\text{Cl}_{12}$ to bulk metals via infinite chains of fused metal octahedra in Gd_2Cl_3 and infinite sheets of fused metal octahedra in ZrCl .¹ Among the late transition metals, palladium is of particular interest since it forms well-defined giant cationic clusters such as $\text{Pd}_{561}\text{L}_{60}(\text{OAc})_{180}$ ($\text{L} = \text{phen}, \text{bipy}$) and $\text{Pd}_{561}(\text{phen})_{60}\text{O}_{60}(\text{PF}_6)_{60}$. Such giant palladium clusters have been characterized by high-resolution transmission electron microscopy, electron diffraction, EXAFS, and small-angle X-ray scattering.² The author has discussed some medium size fused polyhedral palladium carbonyl clusters that may

be considered as intermediate stages between discrete polyhedral palladium clusters and the giant palladium clusters.³

In recent years, Ruck and co-workers⁴ have prepared and characterized structurally a variety of transition metal-centered bismuth clusters including species that may be considered as one-dimensional and two-dimensional metals. These structures provide another opportunity to examine the transition in chemical bonding from molecular metal clusters to bulk metals involving elements in a different part of the periodic table. This paper discusses the chemical bonding in such bismuth cluster structures.

2. Background

The polyhedral structural units in the transition metal-centered bismuth clusters discussed in this paper are closely related to those found in polyhedral boranes^{5–8} and Zintl

* E-mail: rbking@sunchem.chem.uga.edu.

(1) King, R. B. *Inorg. Chim. Acta* **1987**, *129*, 91.

(2) Vargafik, M. N.; Zagorodnikov, V. P.; Stolarov, I. P.; Moiseev, I. I.; Kochubev, D. I.; Likholbov, V. A.; Chuvilin, A. L.; Zamarev, K. I. *J. Mol. Catal.* **1989**, *53*, 315.

(3) King, R. B. *Gazz. Chim. Ital.* **1992**, *122*, 383.

(4) Ruck, M. *Angew. Chem., Int. Ed.* **2001**, *40*, 1182.

(5) Muetterties, E. L.; Knoth, W. H. *Polyhedral Boranes*; Marcel Dekker: New York, 1968.

(6) Williams, R. E. *Inorg. Chem.* **1971**, *10*, 210.

(7) Williams, R. E. *Chem. Rev.* **1992**, *92*, 177.

cluster ions,⁹ which, in many cases, may be regarded as three-dimensional aromatic systems.¹⁰ In such structures, the vertex atoms normally contribute three orbitals of their sp^3 manifold to the skeletal bonding of the polyhedron with the fourth sp^3 orbital bonding to an external group or containing a lone pair. The three internal orbitals are partitioned into two p-like degenerate orbitals “tangential” to the surface of the polyhedron and a unique “radial” orbital directed toward the center of the polyhedron. Pairwise overlap of the twin tangential orbitals results in surface bonding consisting of equal numbers of bonding and antibonding molecular orbital (MO) combinations. Overlap of the radial orbitals leads to a multicenter core bond in the center of the polyhedron.¹⁰ For a deltahedron with n vertices, the surface bonding generates n bonding MOs and n antibonding MOs, and the core bonding generates a single bonding MO and $n - 1$ antibonding MOs. This leads to a total of $n + 1$ skeletal bonding MOs requiring $2n + 2$ skeletal electrons in accord with the Wade–Mingos rules^{11–14} as well as the recently reported more general “*mno*” rules of Jemmis, Balakrishnarajan, and Pancharatna.^{15,16}

A neutral bare bismuth atom in a polyhedral cluster is a donor of three skeletal electrons. Thus, a neutral homoatomic cluster with n bare bismuth vertices would have $3n$ skeletal electrons, which exceeds the $2n + 2$ required by the Wade–Mingos rules. For this reason, bare polyhedral bismuth clusters are generally found as cations¹⁷ as exemplified by tricapped trigonal prismatic Bi_9^{5+} and square antiprismatic Bi_8^{2+} . The bicapped square antiprismatic mixed cluster $Si_2Bi_8^{3+}$ is also known.

The bismuth clusters discussed in this paper differ structurally from the simple deltahedral clusters exhibiting three-dimensional aromaticity⁸ in the following ways.

(1) A transition metal (M) is located in the center of the bismuth polyhedron. This leads to replacement of the single n -center Bi_n core bond in the above three-dimensional aromaticity model¹⁰ by n two-center two-electron ($2c-2e$) M–Bi bonds. The valence electrons of the transition metal are a source of the additional electrons required to form n $2c-2e$ bonds rather than a single n -center Bi_n core bond. The coordination requirements of the transition metal determine the form of the Bi_n polyhedron with Bi_6 octahedra, Bi_7 pentagonal bipyramids or capped trigonal prisms, and Bi_8 square antiprisms or bicapped trigonal prisms being observed in known structures. All of these polyhedra are feasible coordination polyhedra that can be formed by hybrids within the nine-orbital sp^3d^5 manifold accessible to d-block transition metals. In contrast to the polyhedral

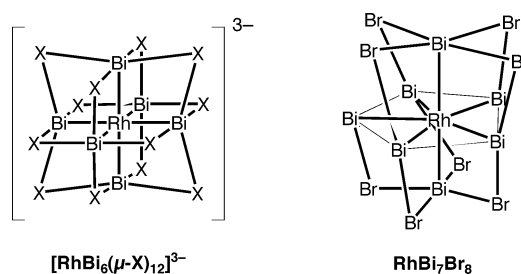


Figure 1. Structures of the $RhBi_6(\mu-X)_{12}^{3-}$ ($X = Br, I$) ions and the $RhBi_7Br_8$ molecule.

boranes, the Bi_n clusters frequently appear to prefer polyhedra having square or rectangular faces. Thus, the square antiprism or bicapped trigonal prism is preferred over the bisdisphenoid for $n = 8$, and the capped trigonal prism sometimes is found rather than the pentagonal bipyramid in $n = 7$ structures.

(2) Another feature of the bismuth clusters discussed in this paper is the addition of halogen atoms so that several of these clusters can be regarded as halogenation products of transition metal bismuthides such as $RhBi_4$ (refs 18 and 19) or $NiBi_3$ (ref 20). The halogen atoms can either form covalent bonds to a portion of the bismuth surface or function as “isolated” negative halide ions simply balancing the charge of positive bismuth clusters. Covalently bonded halogen atoms typically bridge two bismuth atoms.

The bismuth–halogen and bismuth–transition metal bonding noted above use the bismuth valence orbitals more effectively than direct bismuth–bismuth bonding. This can lead to relatively long Bi–Bi edge lengths (>3.4 Å in some cases) in these bismuth cluster polyhedra.

The relative energies of the s and p orbitals of the heavy element bismuth are significantly different than those of the light elements boron and carbon. Thus relativistic effects^{21–24} significantly lower the energy of the bismuth 6s orbitals relative to the 6p orbitals. However, these energy differences do not affect the electron counting discussed in this paper.

3. Discrete Molecular and Ionic Bismuth Clusters

The two types of discrete molecular and ionic transition metal-center bismuth clusters are octahedral $MBi_6(\mu-X)_{12}^{3-}$ ($M = Rh, Ir; X = Br, I$) and pentagonal bipyramidal $RhBi_7(\mu-Br)_8$ (Figure 1). A simple but viable model for the chemical bonding in the octahedral $MBi_6(\mu-X)_{12}^{3-}$ clusters consists completely of localized $2c-2e$ bonds with 24 Bi–X $2c-2e$ bonds and 6 M–Bi $2c-2e$ bonds.²⁵ The chemical bonding in the pentagonal bipyramidal $RhBi_7Br_8$ cluster can be formulated with 16 Bi–X $2c-2e$ bonds, 7 Rh–Bi $2c-2e$ bonds, and a $5c-4e$ bond²⁶ in the equatorial Bi_5 pentagon.²⁵ The equatorial $5c-4e$ bonding in $RhBi_7Br_8$ makes the equatorial Bi_5 unit of the Bi_7 pentagonal bipyramid

(8) King, R. B. *Chem. Rev.* **2001**, *101*, 1119.
 (9) Corbett, J. D. *Chem. Rev.* **1985**, *85*, 383.
 (10) King, R. B.; Rouvray, D. H. *J. Am. Chem. Soc.* **1977**, *99*, 7834.
 (11) Wade, K. *Chem. Commun.* **1971**, 792.
 (12) Mingos, D. M. P. *Nature Phys. Sci.* **1972**, *99*, 236.
 (13) Wade, K. *Adv. Inorg. Chem. Radiochem.* **1976**, *18*, 1.
 (14) Mingos, D. M. P. *Acc. Chem. Res.* **1984**, *17*, 311.
 (15) Jemmis, E. D.; Balakrishnarajan, M. M.; Pancharatna, P. D. *J. Am. Chem. Soc.* **2001**, *123*, 4313.
 (16) Jemmis, E. D.; Balakrishnarajan, M. M.; Pancharatna, P. D. *Chem. Rev.* **2002**, *102*, 93.
 (17) Corbett, J. D. *Prog. Inorg. Chem.* **1976**, *21*, 129.

(18) Alekseevski, N. E.; Zhdanov, G. S.; Zhuravlev, N. N. *Soviet Physics JETP*, **1955**, *1*, 99.
 (19) Glagoleva, V. P.; Zhdanov, G. S. *Sov. Phys. JETP* **1956**, *3*, 155.
 (20) Fjellvåg, H.; Furuseth, S. *J. Less-Common Met.* **1987**, *128*, 177.
 (21) Pitzer, K. S. *Acc. Chem. Res.* **1979**, *12*, 271.
 (22) Pyykkö, P. *Acc. Chem. Res.* **1979**, *12*, 276.
 (23) McKelvey, D. R. *J. Chem. Educ.* **1983**, *60*, 112.
 (24) El-Issa, B. D.; Pyykkö, P.; Zanati, M. *Inorg. Chem.* **1991**, *30*, 2781.
 (25) King, R. B. *J. Chem. Soc., Dalton Trans.* **2003**, 395.
 (26) Xu, Z.; Lin, Z., *Angew. Chem., Int. Ed.* **1998**, *17*, 1686.

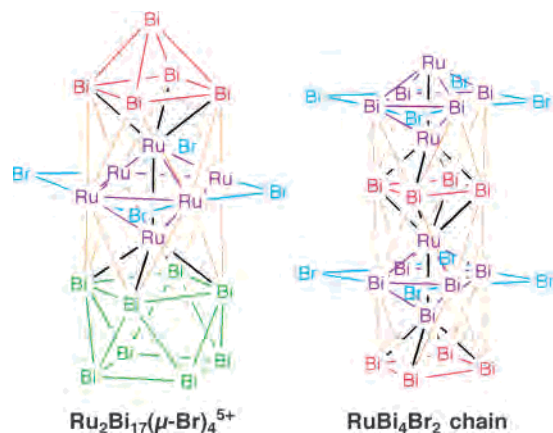


Figure 2. Structures of the $\text{Ru}_2\text{Bi}_{17}(\mu\text{-Br})_4^{5+}$ ion and a segment of the infinite chain found in RuBi_4Br_2 . In the square bipyramidal $\text{Ru}_2\text{Bi}_4(\mu\text{-X})_4$ units common to both structures, the metal (Ru, Bi) atoms are magenta and the $\mu\text{-X}$ atoms are cyan. In $\text{Ru}_2\text{Bi}_{17}(\mu\text{-Br})_4^{5+}$, the Bi_5 square pyramid and the Bi_8 square antiprism are depicted in red and green, respectively.

a Möbius aromatic system.²⁷ The octahedral $\text{MBi}_6(\mu\text{-X})_{12}^{3-}$ anions are found in several types of solid state materials including $\text{Bi}_{14}\text{Si}_2\text{MX}_{12} = [\text{Bi}_8\text{Si}_2^{3+}][\text{MBi}_6(\mu\text{-X})_{12}^{3-}]$ (ref 28), $\text{Bi}_{34}\text{Ir}_3\text{Br}_{37} = [\text{Bi}_6^{4+}][\text{Bi}_5^{3+}]_2[\text{IrBi}_6(\mu\text{-Br})_{12}^{3-}]_2[\text{IrBi}_6(\mu\text{-Br})_{13}^{4-}]$ (ref 29), and other $\text{Bi}_{12-x}\text{MX}_{13-x}$ species.³⁰

4. From a Molecular Cluster to a One-Dimensional Metal: The $\text{Ru}_2\text{Bi}_4(\mu\text{-Br})_4$ Building Block

A phase of composition $\text{Ru}_3\text{Bi}_{24}\text{Br}_{20} = [\text{Ru}_2\text{Bi}_{17}(\mu\text{-Br})_4^{5+}][\text{RuBi}_6(\mu\text{-Br})_{12}^{4-}][\text{BiBr}_4^-]$ is obtained by reaction of bismuth, ruthenium, and BiBr_3 in a sealed, evacuated quartz tube at 450 °C.³¹ The $\text{RuBi}_6(\mu\text{-Br})_{12}^{4-}$ anions in this structure are isoelectronic and isostructural with the $\text{MBi}_6(\mu\text{-X})_{12}^{3-}$ ($\text{M} = \text{Rh}, \text{Ir}$) anions discussed above (Figure 1). The bismuth atoms in the BiBr_4^- anions achieve approximate octahedral geometry by coordination to bromine atoms in the $\text{Ru}_2\text{Bi}_{17}(\mu\text{-Br})_4^{5+}$ units.

Of interest is the nature of the chemical bonding in the $\text{Ru}_2\text{Bi}_{17}(\mu\text{-Br})_4^{5+}$ cluster (Figure 2). The 19 vertices in this cluster can be dissected into square pyramidal Bi_5^{2+} (red in Figure 2), square antiprismatic Bi_8^{3+} (green in Figure 2), and square bipyramidal (ideal D_{4h} symmetry) $\text{Ru}_2\text{Bi}_4(\mu\text{-Br})_4$ units (magenta and cyan in Figure 2). In a given $\text{Ru}_2\text{Bi}_{17}(\mu\text{-Br})_4^{5+}$ cluster, the square bipyramidal $\text{Ru}_2\text{Bi}_4(\mu\text{-Br})_4$ units act as a bridge between the Bi_5^{2+} and Bi_8^{3+} units. One of the ruthenium atoms in the $\text{Ru}_2\text{Bi}_4(\mu\text{-Br})_4$ unit caps the square face of the Bi_5^{2+} square pyramid (red) to form a RuBi_5^{2+} octahedron. The other ruthenium atom in the $\text{Ru}_2\text{Bi}_4(\mu\text{-Br})_4$ unit caps one of the square faces in the Bi_8^{3+} square antiprism (green) to form a RuBi_8^{3+} capped square antiprism. The capped square antiprism is frequently found in bare metal clusters of the group 14 elements, notably E_9^{4-} ($\text{E} = \text{Si}, \text{Ge}, \text{Sn}, \text{Pb}$).^{32,33} In this way, the square bipyramidal $\text{Ru}_2\text{Bi}_4(\mu\text{-Br})_4$ unit is a bifunctional building block linking two clusters by capping their square faces.

In order to count electrons in this species, first consider the bifunctional square bipyramidal $\text{Ru}_2\text{Bi}_4(\mu\text{-Br})_4$ unit. The equatorial Bi_4 square in this unit may be derived from the known³⁴ square Bi_4^{2-} , which may be regarded as a purely inorganic analogue of the cyclobutadiene dianion. A neutral Bi_4 square can function as a four-electron donor to both axial Ru atoms in a Ru_2Bi_4 square bipyramid through multicenter bonds as depicted in Figure 3. Thus, the filled a molecular orbital (MO) of Bi_4 forms a $6c-2e$ core bond with both Ru atoms. Furthermore, the two perpendicular degenerate e MOs of Bi_4 form multicenter π -type bonds with both Ru atoms. The Ru–Ru distance in the $\text{Ru}_2\text{Bi}_4(\mu\text{-Br})_4$ unit³¹ is 2.832(1) Å suggesting a direct Ru–Ru single bond indirectly providing one additional electron for each ruthenium atom. Thus, each Ru vertex in the square bipyramidal $\text{Ru}_2\text{Bi}_4(\mu\text{-Br})_4$ unit receives a total of five electrons from the other five atoms in this unit and therefore is isoelectronic with a $(\eta^5\text{-C}_5\text{H}_5)\text{Ru}$ vertex, which is a donor of one skeletal electron.

The Bi–Bi distance of 2.94 Å in the square dianion³⁴ Bi_4^{2-} lengthens drastically to 3.42 Å in the square bipyramidal $\text{Ru}_2\text{Bi}_4(\mu\text{-Br})_4$ structural unit in the $\text{Ru}_2\text{Bi}_{17}(\mu\text{-Br})_4^{5+}$ cluster.³¹ This is consistent with the expected major reduction of the Bi–Bi bond order for the following reasons in going from a simple Bi_4 square to a $\text{Ru}_2\text{Bi}_4(\mu\text{-Br})_4$ square bipyramid: (1) tetrahapto bonding of a ruthenium atom to each side of the $\text{Bi}_4(\mu\text{-Br})_4$ square; (2) addition of the external edge-bridging bromine atoms.

These Bi–Ru and Bi–Br bonding interactions weaken the direct Bi–Bi interactions thereby lengthening the corresponding Bi–Bi distances.

Considering a square bipyramidal $\text{Ru}_2\text{Bi}_4(\mu\text{-Br})_4$ unit as a link between two clusters donating one skeletal electron to each cluster provides the following electron-counting schemes for the $\text{Bi}_5\text{Ru}^{2+}$ octahedron and the $\text{Bi}_8\text{Ru}^{3+}$ capped square antiprism in the $\text{Ru}_2\text{Bi}_{17}(\mu\text{-Br})_4^{5+}$ cluster:

A. For the $\text{Bi}_5\text{Ru}^{2+}$ octahedron:

The $\text{Ru}_2\text{Bi}_4(\mu\text{-Br})_4$ vertex: $1 \times 1 =$	1 electron
5 bare Bi vertices: $5 \times 3 =$	15 electrons
+2 charge:	–2 electrons
Total skeletal electrons for the $\text{Bi}_5\text{Ru}^{2+}$ octahedron	14 electrons

B. For the $\text{Bi}_8\text{Ru}^{3+}$ capped square antiprism:

The $\text{Ru}_2\text{Bi}_4(\mu\text{-Br})_4$ vertex: $1 \times 1 =$	1 electron
8 bare Bi vertices: $8 \times 3 =$	24 electrons
+3 charge:	–3 electrons
Total skeletal electrons for the $\text{Bi}_8\text{Ru}^{3+}$ capped square antiprism	22 electrons

These skeletal electron counts are in accord with the Wade–Mingos rules^{11–14} and the recently published “*mno*” rules of Jemmis, Balakrishnarajan, and Pancharatna.^{15,16} Thus, 14 skeletal electrons correspond to $2n + 2$ ($n = 6$) for the RuBi_5^{2+} octahedron, the six-vertex *closo* deltahedron. Similarly, 22 skeletal electrons correspond to $2n + 4$ ($n = 9$) for the RhBi_8^{3+} capped square antiprism, a nine-vertex *nido* polyhedron.

(27) Zimmerman, H. E. *Acc. Chem. Res.* **1971**, *4*, 272.

(28) Ruck, M. Z. *Anorg. Allg. Chem.* **2000**, *626*, 14.

(29) Ruck, M. Z. *Anorg. Allg. Chem.*, **1998**, *624*, 521.

(30) Ruck, M.; Hampel, S. *Polyhedron* **2002**, *21*, 651.

(31) Ruck, M. Z. *Anorg. Allg. Chem.* **1997**, *623*, 1591.

(32) Corbett, J. D. *Chem. Rev.* **1985**, *85*, 383.

(33) Fässler, T. F. *Coord. Chem. Rev.* **2001**, *215*, 347.

(34) Cisar, A.; Corbett, J. D. *Inorg. Chem.* **1977**, *16*, 2482.

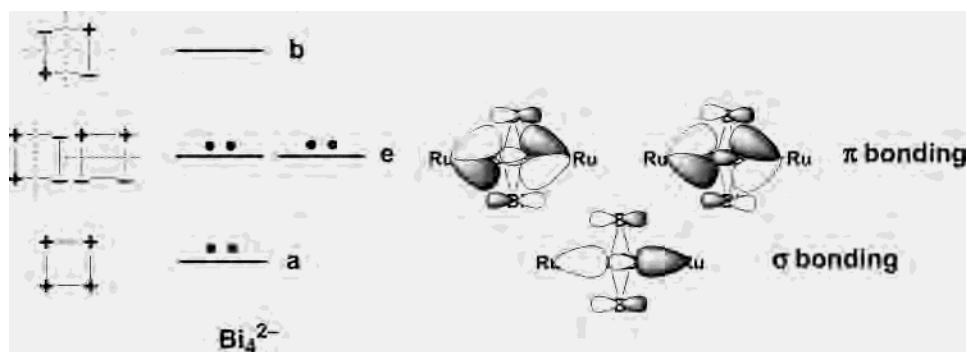


Figure 3. The molecular orbitals in a Bi_4^{2-} square and the involvement of these orbitals in the multicenter bonding found in the square pyramidal $\text{Ru}_2\text{Bi}_4(\mu\text{-X})_4$ unit.

Polymeric species can be obtained by combining difunctional units. In the case of the transition metal-centered bismuth clusters, this can be accomplished by first using the square bipyramidal $\text{Ru}_2\text{Bi}_4(\mu\text{-Br})_4$ unit to cap a Bi_4 square on both the top and bottom to generate a neutral Ru_2Bi_4 octahedron (Figure 2). The free ruthenium atoms of the $\text{Ru}_2\text{Bi}_4(\mu\text{-Bi})_4$ units can then cap additional Bi_4 squares so that this process can be continued indefinitely to give infinite chains of alternating Bi_4 squares and $\text{Ru}_2\text{Bi}_4(\mu\text{-Bi})_4$ units with a limiting stoichiometry RuBi_4Br_2 . Such RuBi_4Br_2 ($\text{X} = \text{Br}, \text{I}$) species can be obtained by direct combination of the elements in the stoichiometric ratios in sealed quartz tubes at $450\text{ }^\circ\text{C}$.³⁵ Each Ru_2Bi_4 octahedron has the 14 skeletal electrons ($= 2n + 2$ for $n = 6$) required by the Wade–Mingos rules^{11–14} as follows:

$2 \text{Ru}_2\text{Bi}_4(\mu\text{-Br})_4$ vertices: $2 \times 1 =$	2 electrons
4 bare Bi vertices: $4 \times 3 =$	12 electrons
Total skeletal electrons for the $\text{Bi}_8\text{Ru}^{3+}$ capped square antiprism	14 electrons

In RuBi_4Br_2 , the ruthenium atoms are localized in pairs with a $\text{Ru}\text{--}\text{Ru}$ bonding distance of 2.854 \AA very similar to that found in the $\text{Ru}_2\text{Bi}_{17}(\mu\text{-Br})_4^{5+}$ cluster discussed above. This is related to the Peierls distortion found in one-dimensional metals.³⁶

The dimensions of the two different types of Bi_4 squares in the structure of RuBi_4Br_2 (Figure 2)³⁵ provide an excellent illustration of the major effects of the bridging bromine atoms on the $\text{Bi}\text{--}\text{Bi}$ distances. Thus, the $\text{Bi}\text{--}\text{Bi}$ distances are 3.38 \AA in the $\text{Ru}_2\text{Bi}_4(\mu\text{-Br})_4$ units of RuBi_4Br_2 with $\mu\text{-Br}$ bridges along each of the four edges of the Bi_4 square (magenta in Figure 2). However, the $\text{Bi}\text{--}\text{Bi}$ edge distances are only 3.06 \AA in the other type of Bi_4 square in RuBi_4Br_2 without $\mu\text{-Br}$ bridges (red in Figure 2).

5. Other Structures with Infinite Chains of MBin Polyhedra

5.1 The $\text{Rh}_3\text{Bi}_{12}\text{Br}_2$ Structure. The intermetallic RhBi_4 is of interest since it has three modifications, two of which exhibit superconductivity below $\sim 3\text{ K}$.^{18,19} The structure of RhBi_4 consists of condensed $\text{RhBi}_{8/2}$ square antiprisms forming two interpenetrating enantiomorphic chiral $3^2 \cdot 10^4$ nets.³⁷

(35) Ruck, M. Z. *Anorg. Allg. Chem.* **1997**, 623, 1583.

(36) Roth, S. *One-dimensional Metals: Physics and Materials Science*; Weinheim: New York, 1995; Chapter 4.

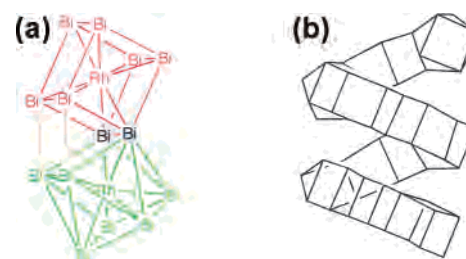


Figure 4. (a) A $\text{RhBi}_{8/2}$ cube (red) joined to an $\text{RhBi}_{8/2}$ square antiprism (green) as found in $\text{Rh}_3\text{Bi}_{12}\text{Br}_2$. (b) A short segment of the helical structure obtained from these building blocks.

An oxidation product of RhBi_4 of stoichiometry $\text{Rh}_3\text{Bi}_{12}\text{Br}_2$ is obtained by heating a mixture of niobium, rhodium, bismuth, and bromine in a sealed quartz tube to $1000\text{ }^\circ\text{C}$.³⁸ The structure of $\text{Rh}_3\text{Bi}_{12}\text{Br}_2$ (Figure 4a) is constructed from infinite chains of alternating $\text{RhBi}_{8/2}$ cubes (red) and square antiprisms (green) sharing common edges. This linkage leads to a natural twist in the resulting chains similar to that found in RhBi_4 . These twisted chains are wound into screws (Figure 4b) that surround the bromide ions, which thus fill the chiral pores of the framework of the $[\text{RhBi}_{8/2}]_\infty$ screws.³⁷ The $[\text{RhBi}_{8/2}]_\infty$ framework may be regarded as cationic with an average positive charge of $2/3$ per rhodium atom.

The bookkeeping of electrons and orbitals in a $\text{RhBi}_{8/2}^+$ building block of the $\text{Rh}_3\text{Bi}_{12}\text{Br}_2$ structure can proceed as follows:

A. Sources of electrons and orbitals

Interstitial rhodium atom: $1 \times 9 =$	9 electrons	9 orbitals
$1/2$ Bismuth atoms: $1/2 \times 3 =$	12 electrons	12 orbitals
+1 Charge:	-1 electron	
Total available electrons and orbitals:	20 electrons	21 orbitals

B. Uses of electrons and orbitals

8 $\text{Rh}\text{--}\text{Bi}$ 2c-2e bonds: $8 \times 2 =$	16 electrons	16 orbitals
$1/2$ $\text{Bi}\text{--}\text{Bi}$ 2c-2e bonds: $1/2 \times 2 =$	4 electrons	4 orbitals
Electrons and orbitals required:	20 electrons	20 orbitals

The following points about this allocation of electrons and orbitals are of interest.

(1) The square antiprismatic hybridization of the central rhodium atom in an $\text{RhBi}_{8/2}^+$ antiprism uses eight of the nine orbitals of the sp^3d^5 rhodium manifold leaving the $\text{d}(z^2)$

(37) Grin, Y.; Wedig, U.; von Schnering, H. G. *Angew. Chem., Int. Ed. Engl.* **1995**, 34, 1204.

(38) Ruck, M. *Solid State Sci.* **2001**, 3, 369.

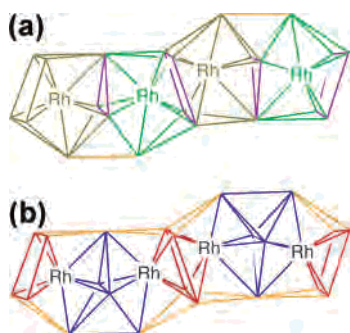


Figure 5. A portion of the $[\text{RhBi}_{7/2}\text{Bi}]_{\infty}$ chains found in $\text{Rh}_2\text{Bi}_9\text{Br}_3$ colored in two different ways with some edges omitted for clarity. (a) The fused $\text{RhBi}_{7/2}\text{Bi}$ bicapped trigonal prisms are colored alternately in light and dark green with the edges of the shared faces (alternating triangles and quadrilaterals) colored in magenta and other edges in orange. (b) The $[\text{RhBi}_{7/2}\text{Bi}]_{\infty}$ chain is shown as a sequence of alternating vertex-sharing Rh_2Bi_4 octahedra (red) and Rh_2Bi_5 pentagonal bipyramids (blue) with other edges in orange.

orbital vacant. The $d(z^2)$ orbitals of adjacent rhodium atoms can overlap providing a mechanism for conductivity. Reduction of the positive charge on a $\text{RhBi}_{8/2}$ unit from $+1$ to $+2/3$ in the actual $\text{Rh}_3\text{Bi}_{12}\text{Br}_2$ corresponds to doping each $d(z^2)$ orbital with $1/3$ electron providing a mechanism for electrical conductivity through electrons in the conduction band.

(2) The electron localization function (ELF) of $\text{Rh}_3\text{Bi}_{12}\text{Br}_2$ indicates that the lone pairs on the bismuth atoms are located at the surfaces of the polyhedra, pointing away from the metallic bonding inside the framework.³⁷ Each bismuth vertex thus provides three rather than five skeletal electrons in accord with the above electron-counting scheme similar to other bare bismuth clusters. The hybridization of the bismuth atoms can be regarded as trigonal sp^2 leaving one extra p orbital from the sp^3 manifold. Two of these sp^2 hybrids of each bismuth atom are used for the $2c-2e$ Bi–Rh bonds leaving the third sp^2 hybrid for the external lone pair. The extra p orbital on each Bi vertex can be used for π -bonding in the Bi_4 squares of the antiprisms or cubes similar to isolated bismuth squares in Bi_4^{2-} (ref 34) or cyclobutadiene. This leads to $4/2$ $2c-2e$ Bi–Bi π bonds for each $\text{RhBi}_{8/2}$ polyhedron as implied by the electron and orbital bookkeeping outlined above.

5.2 The $\text{Rh}_2\text{Bi}_9\text{Br}_3$ Structure. Altering the conditions for the high-temperature Nb/Br/Bi/Rh reaction leads to a material of stoichiometry $\text{Rh}_2\text{Bi}_9\text{Br}_3$. Analogous species can also be obtained with iridium rather than rhodium and iodine rather than bromine.³⁹ The structure of this product contains chains of $\text{RhBi}_{7/2}\text{Bi}$ bicapped trigonal prisms linked alternately through quadrilateral and triangular faces (Figure 5a). The bromine atoms are ionic so that each $\text{RhBi}_{7/2}\text{Bi}$ building block has an average charge of $+3/2$. Unlike the $\text{Rh}_3\text{Bi}_{12}\text{Br}_2$ structure, one of the bismuth atoms in each $\text{RhBi}_{7/2}\text{Bi}$ bicapped trigonal prism is unique to that building block (Bi(4) in ref 39). These bismuth atoms in adjacent $\text{RhBi}_{7/2}\text{Bi}$ bicapped trigonal prisms are close enough to form a $2c-2e$ Bi–Bi bond (orange in Figure 5a).

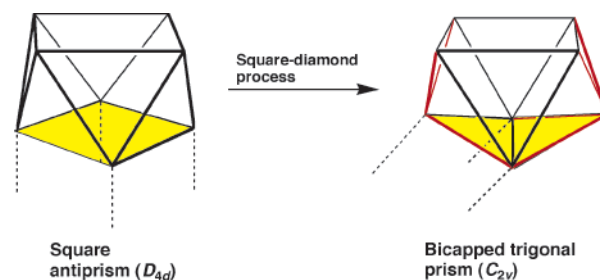


Figure 6. The square-diamond process converting a square antiprism into a bicapped trigonal prism. The face involved in this square-diamond process is colored yellow, the edges to the capping vertices in the bicapped trigonal prism are colored red, and the points of fusion to an adjacent similar polyhedron are indicated by dashed lines.

The $\text{RhBi}_{7/2}\text{Bi}$ bicapped trigonal prism building block found in $\text{Rh}_2\text{Bi}_9\text{Br}_3$ is closely related to a square antiprism by a single square-diamond process on one of the square faces (Figure 6). Thus, one of the square faces of each square antiprism becomes a pair of triangular faces in the corresponding bicapped trigonal prism (depicted in yellow in Figure 6). One of these two triangular faces links two adjacent $\text{RhBi}_{7/2}\text{Bi}$ polyhedra (depicted in magenta in Figure 5a).

For the purpose of electron and orbital bookkeeping in $\text{Rh}_2\text{Bi}_9\text{Br}_3$, it is instructive to use an alternative geometrical view of the structure (Figure 5b) as alternating Rh_2Bi_4 octahedra (red) and Rh_2Bi_5 pentagonal bipyramids (blue). Note that the rhodium vertices are equatorial rather than axial vertices of the pentagonal bipyramids. The Rh_2Bi_4 octahedra are closely related to the square bipyramidal $\text{Ru}_2\text{Bi}_4(\mu\text{-Br})_4$ units discussed in the previous section. Their rhodium vertices each analogously provide one skeletal electron for the Rh_2Bi_5 pentagonal bipyramids leading to the following skeletal electron counting scheme for the latter considered as monocations Rh_2Bi_5^+ because of the bromide counterions in $\text{Rh}_2\text{Bi}_9\text{Br}_3$:

2 Rh_2Bi_4 vertices: $2 \times 1 =$	2 electrons
5 bare Bi vertices: $5 \times 3 =$	15 electrons
+1 charge	–1 electron
<i>Total skeletal electrons for the Rh_2Bi_5^+ pentagonal bipyramid</i>	<i>16 electrons</i>

This skeletal electron count is in accord with the Wade–Mingos rules^{11–14} requiring 16 skeletal electrons ($=2n + 2$ for $n = 7$) for a seven-vertex deltahedron such as the pentagonal bipyramid.

6. Structures with Infinite Layers of MBi_n Polyhedra

6.1 The $\text{Pt}_3\text{Bi}_{13}\text{I}_7$ Structure. Reaction of bismuth, BiI, and PtI_2 in a sealed tube at 360 °C for several weeks gives a black solid of stoichiometry $\text{Pt}_3\text{Bi}_{13}\text{I}_7$.⁴⁰ X-ray diffraction of this material indicates a structure consisting of alternating layers of Kagomé nets of $\text{PtBi}_{8/2}$ cubes (Figure 7), iodine atoms, and $\text{BiI}_{4/2}\text{I}_2^-$ zigzag chains with overall composition $[\text{PtBi}_{8/2}]_3[\text{BiI}_{4/2}\text{I}_2][\text{I}]_3$. Assuming the usual oxidation states of $+3$ for bismuth and -1 for iodine leads to a $+4/3$ charge on each $\text{PtBi}_{8/2}$ cube.

(39) Ruck, M.; Heich, R. M. *Z. Anorg. Allg. Chem.* **2000**, 626, 2449.

(40) Ruck, M. *Z. Anorg. Allg. Chem.* **1997**, 623, 1535.

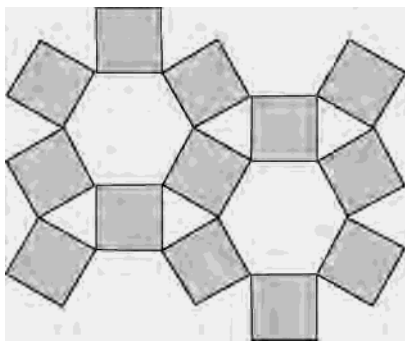


Figure 7. A “top” view of the Kagomé net of $\text{PtBi}_{8/2}$ cubes found in $\text{Pt}_3\text{Bi}_{13}\text{I}_7$ with the top faces of the Pt-filled cubes indicated in gray.

The electron and orbital bookkeeping in a neutral $\text{PtBi}_{8/2}$ unit is analogous to that discussed above for the $\text{RhBi}_{8/2}^+$ unit in $\text{Rh}_3\text{Bi}_{12}\text{Br}_2$ as follows:

A. Sources of electrons and orbitals

Interstitial platinum atom:	10 electrons	9 orbitals
$\frac{1}{2}$ Bismuth atoms: $\frac{1}{2} \times 3 =$	12 electrons	12 orbitals
<i>Total available electrons and orbitals:</i>	<i>22 electrons</i>	<i>21 orbitals</i>

B. Uses of electrons and orbitals

8 Pt–Bi 2c–2e bonds: $8 \times 2 =$	16 electrons	16 orbitals
Ninth Pt orbital in the sp^3d^5 manifold with a lone pair	2 electrons	1 orbital
$\frac{1}{2}$ Bi–Bi 2c–2e bonds: $\frac{1}{2} \times 2 =$	4 electrons	4 orbitals
<i>Electrons and orbitals required:</i>	<i>22 electrons</i>	<i>21 orbitals</i>

Note that after forming the eight 2c–2e bonds with the bismuth atoms of the $\text{PtBi}_{8/2}$ cube each platinum atom has a ninth orbital (probably the $d(z^2)$ orbital) which can contain a lone electron pair in accord with this electron/orbital bookkeeping scheme. However, partial oxidation of the $\text{PtBi}_{8/2}$ unit by removal of an average of $\frac{4}{3}$ electrons per unit in accord with the $\text{Pt}_3\text{Bi}_{13}\text{I}_7$ stoichiometry can remove some of the electron density from this orbital corresponding to holes in the valence band.

6.2 The $\text{Ni}_4\text{Bi}_{12}\text{X}_3$ and $\text{Ni}_4\text{Bi}_{13}\text{X}_6$ ($\text{X} = \text{Br}, \text{I}$) Structures.

Reaction of bismuth, nickel, and iodine in a sealed quartz tube at 440 °C over two weeks gives a mixture of phases of nominal stoichiometry $\text{Ni}_4\text{Bi}_{12}\text{I}_3$ and $\text{Ni}_4\text{Bi}_{13}\text{I}_6$ (more precisely $\text{Ni}_4\text{Bi}_{12.86}\text{I}_6$) shown by X-ray diffraction to have the same nickel-centered bismuth cluster network with covalently bonded halogens.⁴¹ The corresponding bromide $\text{Ni}_4\text{Bi}_{13}\text{I}_6$ is analogously made from bismuth, nickel, and either bromine or BiBr_3 as the bromine source.⁴² These Ni/Bi/X clusters may be regarded as oxidation (halogenation) products of the known²⁰ NiBi_3 , which has a very similar nickel-centered bismuth cluster network and which exhibits superconducting properties.⁴³

The $\text{NiBi}_{6/3}\text{Bi}$ building blocks in these structures consist of nickel-centered Bi_7 capped trigonal prisms, which are first joined into infinite $[\text{NiBi}_{6/3}\text{Bi}]_\infty$ chains by sharing rectangular faces (Figure 8a). In these $[\text{NiBi}_{6/3}\text{Bi}]_\infty$ chains, six of the seven bismuth vertices of a given Bi_7 capped trigonal prism are shared by three capped trigonal prisms (blue in Figure

8a) whereas the seventh bismuth vertex (the capping vertex, red in Figure 8a) is unique to a single capped trigonal prism. The nickel atoms inside these capped trigonal prisms form zigzag chains with Ni–Ni bonding distances of 2.51 Å (green in Figure 8a). These infinite $[\text{NiBi}_{6/3}\text{Bi}]_\infty$ chains form infinite corrugated layers (Figure 8b) in which the capping vertices in two adjacent chains form empty trigonal prismatic cavities with the adjacent noncapping bismuth vertices. Each of the capping vertices, namely the vertices unique to a single capped trigonal prism in a given $[\text{NiBi}_{6/3}\text{Bi}]_\infty$ chain, forms Bi–Bi bonds to two bismuth atoms in adjacent $[\text{NiBi}_{6/3}\text{Bi}]_\infty$ chains (orange in Figure 8b).

The bonding of the halogen atoms to the $\text{NiBi}_{6/3}\text{Bi}$ units is somewhat complicated since there are a variety of slightly different Bi–X distances. Thus in $\text{Ni}_4\text{Bi}_{12}\text{I}_3$ the Bi–I distances below 4.0 Å are 3.37, 3.44, 3.55, 3.69, 3.78, and 3.84 Å. If Bi–I distances of 3.55 Å and shorter are assumed to be bonding distances and those larger assumed to be nonbonding distances, then each iodine atom can very roughly be considered to bridge two bismuth atoms. However, the Bi–I distances of 3.69, 3.78, and 3.84 Å are short enough to suggest weaker metal–halogen bonding. Because of this complication, electron counting procedures in these clusters have limited reliability. However, if only the fused nickel-centered bismuth polyhedra are considered then the electron counting in an $\text{NiBi}_{6/3}\text{Bi}$ unit can be summarized as follows:

A. Source of electrons and orbitals

1 Ni vertex in the center	10 electrons	9 orbitals
$\frac{1}{3} + 1 = 3$ bare Bi vertices: $3 \times 3 =$	9 electrons	9 orbitals
<i>Total skeletal electrons and orbitals available in a $\text{NiBi}_{6/3}\text{Bi}$ unit</i>	<i>19 electrons</i>	<i>18 orbitals</i>

B. Use of electrons and orbitals

7 Ni–Bi 2c–2e bonds: $7 \times 2 =$	14 electrons	14 orbitals
$\frac{1}{2}$ Ni–Ni 2c–2e bonds: $\frac{1}{2} \times 2 =$	2 electrons	2 orbitals
$\frac{1}{2}$ Bi–Bi 2c–2e bonds: $\frac{1}{2} \times 2 =$	2 electrons	2 orbitals
<i>Total skeletal electrons required for a $\text{NiBi}_{6/3}\text{Bi}$ unit</i>	<i>18 electrons</i>	<i>18 orbitals</i>

The following points about this electron-counting scheme are of interest.

(1) The nickel atoms use all nine orbitals of their sp^3d^5 manifolds to form seven 2c–2e Ni–Bi bonds to the bismuth vertices of the surrounding capped trigonal prism and two 2c–2e Ni–Ni bonds to the adjacent nickel atoms in the Ni_n zigzag chain. The coordination geometry of the nickel atoms is a tricapped trigonal prism like the discrete ion⁴⁴ ReH_9^{2-} . This coordination polyhedron is possible with a sp^3d^5 manifold without the need for f orbitals.

(2) The six bismuth atoms forming each $\text{NiBi}_{6/3}$ trigonal prism are each shared between three trigonal prisms, and thus, each such bismuth atom forms three Ni–Bi 2c–2e bonds. Three of the four orbitals of the sp^3 manifolds of each of these bismuth atoms are thus used for the Ni–Bi 2c–2e bonds leaving the fourth orbital for the lone pair.

(3) The seventh bismuth atom, namely the bismuth atom capping a rectangular face of the underlying $\text{NiBi}_{6/3}$ trigonal prism, is bonded to only one nickel atom. The remaining

(41) Ruck, M. Z. *Anorg. Allg. Chem.* **1997**, 623, 243.

(42) Ruck, M. Z. *Anorg. Allg. Chem.* **1999**, 625, 453.

(43) Fujimori, Y.; Kan, S.; Shinozaki, B.; Kawaguti, T. *J. Phys. Soc. Jpn.* **2000**, 69, 3017.

(44) Abrahams, S. C.; Ginsberg, A. P.; Knox, K. *Inorg. Chem.* **1964**, 3, 558.

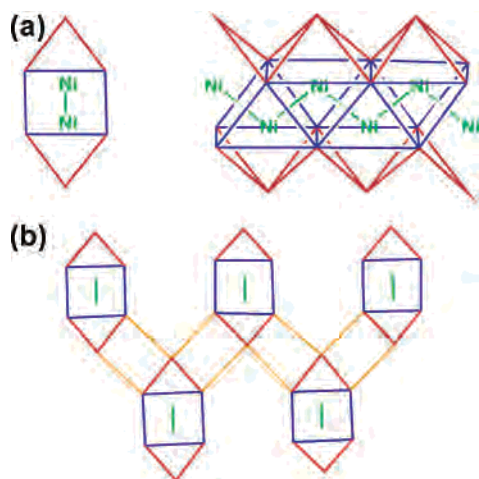


Figure 8. (a) Two views of a portion of the $[\text{NiBi}_{6/3}\text{Bi}]_{\infty}$ chains found in $\text{Ni}_4\text{Bi}_{12}\text{X}_3$ and $\text{Ni}_4\text{Bi}_{13}\text{X}_6$ structures. (b) Joining these $[\text{NiBi}_{6/3}\text{Bi}]_{\infty}$ chains into a corrugated layer structure. The nickel zigzag chains in these structures are shown in green, the trigonal prisms in blue, the edges to the capping bismuth atom in red, and the new Bi–Bi edges connecting the chains into a corrugated layer in orange.

two internal orbitals are available to form Bi–Bi bonds with bismuth atoms in $\text{NiBi}_{6/3}\text{Bi}$ capped trigonal prisms of adjacent chains (orange in Figure 8b) thereby creating the corrugated layer structure of $\text{Ni}_4\text{Bi}_{12}\text{X}_3$.

7. Summary

The chemical bonding in many of the ternary transition metal-centered bismuth cluster halides is related to that in

the deltahedral boranes exhibiting three-dimensional aromaticity by replacing the multicenter core bond in the boranes with $2c-2e$ bonds from the central transition metal to the bismuth atom. Examples of discrete transition metal-centered bismuth cluster molecules or ions are octahedral $\text{MBi}_6(\mu\text{-X})_{12}^{z-}$ ($\text{X} = \text{Br}, \text{I}$; $\text{M} = \text{Rh}, \text{Ir}$, $z = 3$; $\text{M} = \text{Ru}$, $z = 4$) with exclusively $2c-2e$ bonds and pentagonal bipyramidal RhBi_7Br_8 with a $5c-4e$ bond in the equatorial plane suggestive of Möbius aromaticity. The compound $\text{Ru}_3\text{Bi}_{24}\text{Br}_{20}$ contains a more complicated discrete bismuth cluster ion $\text{Ru}_2\text{Bi}_{17}(\mu\text{-Br})_4^{5+}$, which can be dissected into a RuBi_5 *closo* octahedron and a RuBi_8 *nido* capped square antiprism bridged by a $\text{Ru}_2\text{Bi}_4(\mu\text{-Br})_4$ structural unit. In RuBi_4X_2 ($\text{X} = \text{Br}, \text{I}$) the same $\text{Ru}_2\text{Bi}_4(\mu\text{-Br})_4$ structural unit bridges Bi_4 squares to give infinite chains of Ru_2Bi_4 octahedra. The electron counts of the RuBi_5 , RuBi_8 , and Ru_2Bi_4 polyhedra in these structures follow the Wade–Mingos rules. A different infinite chain structure is constructed from fused $\text{RhBi}_{7/2}\text{Bi}$ bicapped trigonal prisms in $\text{Rh}_2\text{Bi}_9\text{Br}_3$. This $\text{Rh}_2\text{Bi}_9\text{Br}_3$ structure can alternatively be derived from alternating $\text{Rh}_{2/2}\text{Bi}_4$ octahedra and $\text{Rh}_{2/2}\text{Bi}_5$ pentagonal bipyramids with electron counts obeying the Wade–Mingos rules. Related chemical bonding principles appear to apply to more complicated layer structures such as $\text{Pt}_3\text{Bi}_{13}\text{I}_7$ and $\text{Ni}_4\text{Bi}_{12}\text{X}_3$.

Acknowledgment. I am indebted to the National Science Foundation for partial support of this work under Grant CHE-0209857.

IC030210N